We appreciate two anonymous reviewers' constructive comments. Here are the line-by-line responses.

Anonymous Referee #5

This manuscript presented a detailed analysis on radical levels at a rural site around Seoul based on an observational dataset and box models. The observational data on HONO and VOCs is interesting, and gave valuable insight into the HONO concentration in Korea. The results gave lend insight into radical recycle. This manuscript should be of interest to ACP readers and would be suitable for publication with minor revisions.

1. Line 170-172. The author used a Thermo 42i TL to observe NO/NOx. I am afraid that NO2 measurements systematically overestimate the true value because of interferences of these compounds especially when Sampling photochemicallly aged air masses. The Mo converter could other oxidized nitrogen compounds such as peroxyacetyl nitrate and nitric acid are also partly converted to NO. The author should discuss the uncertainties on results caused by NO/NO2 observations.

In the method section (2.1) and the result section (3.3), we clearly mentioned about the potential systematic overestimation as the reviewer suggested with proper referencing.

2. The author mentioned that TRF is not directly influenced by Seoul pollution plume by comparing NO2 concentrations at two sites. This is not enough. In some cases, although NO2 is not transported, other chemical compounds like PAN and nitrate are likely transported a longer distance. The author had better examine the wind direction and velocity. If the manuscript can provide TRF is not located in the downwinded site of Seoul but prevailed winds, the statement will be more evident.

It should be also noted that not all of NO_X is converted to reservoir species such as peroxyacyl nitrates (PANs) or alkylnitrates. PANs usually serve as a reservoir species for long-range transport processes involved with free tropospheric transport, as their chemical lifetime gets longer in low temperature environments. As TRF is located only 3o km away from the city center, highlighting PANs as a significant NO_X sources is not appeared to be reasonable.

Previous studies found that he Heterogeneous chemistry on HONO and HNO3 is important on NOx and O3 chemistry. In particular, radicals like OH and HO2 are mostly affected by O3 and NOx. Thus, discussion on Heterogeneous chemistry should be discussed.

We added the discussion about recently found HONO sources from heterogeneous chemical processes in the revised manuscript.

Page 396 . "is about 40 times" should be "are about 40 times".

We corrected as suggested in the revised manuscript.

Line 389 "the impacts to" should be "the impacts on"

We corrected as suggested in the revised manuscript.

Anonymous Referee #4

The manuscript has been improved mainly by employing up-to-date consensus knowledge of the HOx-isoprene chemistry. However still some revision is necessary:

1. Title: Although isoprene chemistry is heavily studied here, roles of anthropogenic hydrocarbon are almost unstudied. Therefore, "urban-rural interactions govern ... " in the current title is too much. "Impact of isoprene and HONO chemistry on ozone and OVOC formation in a semirural South Korean forest" might be better.
We corrected the title as suggested in the revised manuscript.

2. My previous request to mention observation or assumption of J values is neglected. Please include some explanation.
We included an extensive discussion about the photostationary state in the resubmitted manuscript to discuss the point the referee raised about J. The calculated J is based on the assumption that photostationaly state is valid for all time but as we discussed it is not necessarily that the photostationary state is hold even in the remote region as discussed. As the referee suggested, it could be caused by the interferences on observed NO2 due to the Mo-converter. We also included the discussion in the resubmitted manuscript.

3. Now the authors conclude that impact of isoprene chemistry on OH/HO2/RO2 radicals is less important than the impact of the HONO treatment. But still, most description in Introduction is on isoprene chemistry, and HONO is almost unmentioned. More balanced Introduction section is necessary.
We added descriptions on the potential importance of HONO in radical cycle in the introduction.

4. Line 153. Maybe 2012?
It is actually 2013. However, we realized that there is some confusion in notating the observation year. We re-read the whole manuscript and made sure that the year is corrected notated as 2013.

5. How will the possible interference of PANs etc in the NO2 measurement, now mentioned in sections 2.2 and 3.1, affect the discussion on 2P(H2O2)/P(HNO3)? P(HNO3) should be largely affected. Discussion on this point is also critical.
We added discussion on uncertainty that can be caused by the systematically overestimated NO2. If we assume ~ 50% of NO2 overestimation, the ratio will be doubled. Therefore the NOX and VOC limited regime border will set on 0.5. Still, our findings would not be significantly affected.

6. line 402. four different model scenarios
We corrected the typo as suggested.

7. lines 448-449. In Table 3 the authors discussed that HO2 is slightly increased and RO2 is decreased. Why the RO2+HO2 reaction rates increased here?
We rephrase the sentence to reflect the model calculated and analysis results.

8. line 452. Considering relatively high NOx concentrations at TRF, this is surprising …
We think so too. That is why we extensively discussed about it in the manuscript. The critical fact is that NO was observed quite low in the afternoon.

9. lines 499. For more rural condition at the top of Mt. Tai, China, Kanaya et al. (ACP 2009) mentioned that ozone production is basically NOx limited.
We included the reference with a proper introduction in the revised manuscript.

10. line 519. Some more explanation is necessary for the lower P(peroxide)/P(HNO3). Previously in Figure 4, the authors mentioned that P(peroxide) is increased in Scenario 2. Here, the authors mean that P(HNO3) is MORE ENHANCED because of high OH in this scenario, resulting in the LOWER P(peroxide)/P(HNO3)?
As the referee commented in the line item 7, there were some miss-statements about the radical distributions from the different model scenarios. In the revised manuscript, both analysis results are consistently described.

11. line 558. Where did the author discuss on the "factor of 2-3" missing OH reactivity for this campaign?
In the revised manuscript, we did not include this quantitative statement, which may cause confusion.

12. line 560, SOA, not VOCs
We corrected the typo in the revised manuscript.

Impact of isoprene and HONO chemistry on ozone and OVOC formation in a semirural South Korean forest

[1]Saewung Kim, [2]So-Young Kim, [3]Meehye Lee, [3]Heeyoun Shim, [4,5]Glenn M. Wolfe, [6]Alex B. Guenther, and [1]Amy He, [2]Youdeog Hong, [2]Jinseok Han

1 Department of Earth System Science, School of Physical Sciences, University of California, Irvine, Irvine California, 92697 U.S.A.
2 National Institute Environmental Research, Incheon, South Korea
3 Department of Earth and Environmental Sciences, Korean University, Seoul, South Korea
4 Joint Center for Earth Systems Technology, University of Maryland Baltimore County, Baltimore, MD, USA
5 Atmospheric Chemistry and Dynamics Laboratory, NASA Goddard Space Flight Center, Greenbelt, MD, USA
6 Atmospheric Sciences and Global Change Division, Pacific Northwest National Laboratory, Richland WA USA

To be submitted to Atmospheric Chemistry and Physics "East Asian Megacity" Special Issue

Saewung Kim 3/26/2015 10:09 AM
Formatted: Font:(Default) Arial, 14 pt

Saewung Kim 3/26/2015 10:09 AM
Formatted: Centered

Saewung Kim 3/26/2015 10:09 AM
Deleted: Urban-rural interactions govern ozone and oxygenated volatile organic compound formation in a South Korean forest

Saewung Kim 3/26/2015 10:09 AM
Formatted: Font:(Default) Arial

Saewung Kim 3/26/2015 10:09 AM
Formatted: Font:14 pt

Abstract

Rapid urbanization and economic development in East Asia in past decades has led to photochemical air pollution problems such as excess photochemical ozone and aerosol formation. Asian megacities such as Seoul, Tokyo, Shanghai, Gangzhou, and Beijing are surrounded by densely forested areas and recent research has consistently demonstrated the importance of biogenic volatile organic compounds (VOCs) from vegetation in determining oxidation capacity in the suburban Asian megacity regions. Uncertainties in constraining tropospheric oxidation capacity, dominated by hydroxyl radical, undermine our ability to assess regional photochemical air pollution problems. We present an observational dataset of CO, NO_X, SO_2, ozone, HONO, and VOCs (anthropogenic and biogenic) from Taehwa Research Forest (TRF) near the Seoul Metropolitan Area (SMA) in early June 2012. The data show that TRF is influenced both by aged pollution and fresh BVOC emissions. With the dataset, we diagnose HOx (OH, HO_2, and RO_2) distributions calculated using the University of Washington Chemical Box Model (UWCM v 2.1) with near-explicit VOC oxidation mechanisms from MCM 3.2 (The Master Chemical Mechanism). Uncertainty from unconstrained HONO sources and radical recycling processes highlighted in recent studies is examined using multiple model simulations with different model constraints. The results suggest that 1) different model simulation scenarios cause systematic differences in HO_X distributions especially OH levels (up to 2.5 times) and 2) radical destruction (HO_2+HO_2 or HO_2+RO_2) could be more efficient than radical recycling (RO_2+NO) especially in the afternoon. Implications of the uncertainties in radical chemistry are discussed with respect to ozone-VOC-NO_X sensitivity and VOC oxidation product formation rates. Overall, the NO_X limited regime

is assessed except for the morning hours (8 am to 12 pm) but the degree of sensitivity can significantly vary depending on the model scenarios. The model results also suggest that RO_2 levels are positively correlated with oxygenated VOCs (OVOCs) production that is not routinely constrained by observations. These unconstrained OVOCs can cause higher than expected OH loss rates (missing OH reactivity) and secondary organic aerosol formation. The series of modeling experiments constrained by observations strongly urge observational constraint of the radical pool to enable precise understanding of regional photochemical pollution problems in the East Asian megacity region.

1. **Introduction**

NOx ($NO+NO_2$) and volatile organic compounds (VOCs) are two important precursors that drive HOx radical cycles(Levy, 1971). In the presence of NO_X, VOC oxidation processes recycle OH and produce photochemical oxidation products such as ozone and oxygenated VOCs (OVOCs). This reaction cycle is highly non-linear. For example, excess NO_2 may expedite nitric acid formation (R1), limiting ozone production. In the same context, excess VOCs may expedite peroxy radical production (R2), which limits OH regeneration from peroxy radicals.

$$OH + NO_2 + M \rightarrow HNO_3 + M \quad (R1)$$

$$HO_2 + RO_2 \rightarrow ROOH \quad (R2)$$

The non-linearity in tropospheric photochemistry has been relatively well studied in the urban regions of developed countries and applied in ozone reduction policy. The Los Angeles Metropolitan Area has accomplished significant ozone reduction by implementing aggressive emission reductions of both NOx and VOC especially from mobile sources (Ryerson et al., 2013). The remarkable ozone abatement was possible due to the fact that there is no significant pollution transport from other metropolitan areas and no significant natural emission sources especially volatile organic compounds from vegetation (BVOCs; biogenic volatile organic compounds) compared with anthropogenic VOC mostly from mobile sources (Pollack et al., 2013;Huang et al., 2013). In the late 80s, Trainer et al. (1987) first demonstrated the importance of isoprene (C_5H_8) as a peroxy radical source that can contribute significant ozone production in rural areas. The

importance of isoprene in ozone production in urban areas has also been highlighted, e.g. in the Atlanta Metropolitan Area (Chameides et al., 1988).

Isoprene is a hemiterpenoid species and is the globally dominant VOC emission from vegetation (Arneth et al., 2011;Guenther, 2013). Arguably, isoprene is the most frequently studied BVOC from the perspective of atmospheric oxidation processes and their implications for ozone and aerosol formation. However, significant uncertainty hinders assessing the roles of isoprene in regional and global photochemistry in three fronts. First, there is still significant uncertainty in estimating emission rates from each individual plant species on regional scales (Guenther, 2013). Second, limited isoprene inter-comparison results (Barket et al., 2001) suggest that there are large systematic biases among different analytical techniques. Lastly, recent laboratory, theoretical and field observations suggest significant uncertainty in tropospheric isoprene oxidation processes initiated by OH. Until early 2000, it was thought that three first generation isoprene oxidation products (methyl vinyl ketone, methacrolein, and formaldehyde) from OH oxidation were enough to constrain isoprene tropospheric oxidation processes for modeling purposes (e.g. Spaulding et al. (2003) and Dreyfus et al. (2002)). This is an interesting evolution of thoughts considering that Paulson and Seinfeld (1992), one of pioneering works describing isoprene oxidation, clearly claimed that 22 % of first generation isoprene oxidation products from the reaction with OH was not identified and likely included multifunctional C5 compounds. Recent advances in analytical techniques (Kim et al., 2013a) have shown that indeed significant C5-hydroxy carbonyl (e.g. isoprene hydroperxyenals, HPALD) and peroxide compounds are produced as first generation isoprene oxidation products (Crounse et al., 2011;Paulot et al., 2009;Wolfe et

al., 2012;Zhao and Zhang, 2004). The product yields appeared to be a strong function of NO concentrations (Peeters and Muller, 2010). In general, at low to intermediate NO levels (~ 100 pptv or lower), the yields of C5-hydroxy carbonyl compounds become higher. These new findings in the isoprene oxidation process are also closely related with recent findings in unexpectedly high OH concentrations (Hofzumahaus et al., 2009;Lelieveld et al., 2008) and substantial missing OH sinks also known as unexpectedly high OH reactivity in high isoprene environments (Di Carlo et al., 2004;Edwards et al., 2013;Kim et al., 2011;Lou et al., 2010).

These new findings have significant implications for regional air quality especially regarding photochemical ozone and SOA production. Despite the strong anthropogenic pollutant emissions in East Asia (China, Japan and South Korea), recent research has shown that isoprene accounts for a major OH chemical sink in suburban areas near Beijing (Ran et al., 2011), the Pearl River Delta region (Lu et al., 2012), Taipei (Chang et al., 2014) and Seoul (Kim et al., 2013d;Kim et al., 2013b). Consequently, modeling studies also clearly show that isoprene contributes significantly to ozone formation in Asian megacity regions. Kim et al. (2013d) reported that simulated ozone levels with isoprene chemistry are up to 30 % higher than ozone simulation without isoprene chemistry using the WRF-Chem model, indicating an urgent need to implement improved isoprene chemistry schemes in these models in order to simulate the unexpected higher levels of OH in isoprene rich environments. This could become an especially serious issue as Hofzumahaus et al. (2009) reported significantly higher (~ 2.6 times at noon) than expected OH levels in the Pearl River Delta region in China. Therefore, the current assessments based on the conventional OH photochemistry could

significantly misdiagnose regional air-quality status and mislead policy implementation to reduce photochemical air pollution in the East Asian region. Furthermore, as the importance of BVOC in regional air-quality issues in ozone and SOA formation has been also highlighted in Europe and North America, the uncertainty in isoprene photochemistry has significant implications in urban and suburban air quality in general (Zhang et al., 2008a;Sartelet et al., 2012). It should be also noted that HONO has been observed in high-levels in the East Asian region even in the daytime (~ hundreds ppt, (Song et al., 2009;Hao et al., 2006;Li et al., 2012)). The data analysis has consistently indicated that well-known HONO sources cannot account the observed level. Therefore, the implications of HONO as a radical source should also be comprehensively addressed.

We present atmospheric observations of NO_X, CO, VOCs, ozone, and HONO in the Taehwa Research Forest (TRF) in the Seoul Metropolitan Area (SMA), South Korea. We use observed data from June, 2013 to conduct observationally constrained box model (University of Washington Chemical Box Model; UWCM) calculations to estimate OH, HO_2 and RO_2 concentrations with different sets of observational parameters. We discuss current uncertainty in OH-isoprene photochemistry with perspectives of constraining photochemical ozone production and OVOCs precursors of secondary organic aerosols in addition to the roles of unconstrained HONO sources in radical distributions.

2. **Methods**

The Taehwa Research Forest (TRF) is located ~ 35 km from the center of Seoul, South Korea. The TRF is located at the southeastern edge of the Seoul metropolitan Area (SMA, population of ~ 23 million). TRF has a sampling tower located in the middle of a

171 coniferous tree plantation (200 m by 200 m) with the canopy height of 18 m (*Pinus*
172 *koraiensis*) surrounded by a deciduous forest mostly composed by oak. The TRF
173 instrumentation has previously been described by Kim et al. (2013d) along with the
174 previous trace gas observational results. Therefore, just brief descriptions of analytical
175 techniques are given in this paper.
176
177 **2.1. CO, NO_X, SO_2, ozone, VOCs, and meteorological parameters**
178 Thermo Fisher Scientific Enhanced Trace Level Gas Analyzers are used for CO,
179 NO_X, SO_2, and ozone observations as summarized Table 1. A molybdenum (Mo)
180 converter is used to convert NO_2 to NO for the NO_X analyzer. Although Mo converters
181 are still widely used for NO_2 observations, some of thermally unstable oxygenated
182 reactive nitrogen compounds, especially peroxyacyl nitrates, could be also converted to
183 NO_2 by a Mo-converter (Villena et al., 2012). VOC observations are conducted by a
184 High-Sensitivity Proton Transfer RPANeaction-Mass Spectrometer (PTR-MS, Ionicon
185 GmbH). The atmospheric application of this technique is thoroughly reviewed by de
186 Gouw and Warneke (2007). In addition, the instrument suite at TRF is thoroughly
187 described in (Kim et al., 2013d). PTR-MS can quantify atmospheric VOCs that have
188 higher proton affinity than the proton affinity of H_2O (691 kJ mol^{-1}). Most alkanes have
189 lower proton affinity than water but alkene, aromatic and some OVOCs have higher
190 proton affinity and are suitable for quantification using PTR-MS (Blake et al., 2009).
191 These compounds are more reactive than alkane compounds so PTR-MS has capability to
192 observe reactive atmospheric compounds. The TRF PTR-MS system was set to measure
193 acetaldehyde, acetone, acetic acid, isoprene, methylvinylketone (MVK) + methacrolein

194 (MACR), MEK, benzene, xylene (*p*, *m*, and *o*), and monoterpenes (MT). Each compound
195 was set to be monitored for 1 second each resulting in a sample cycle of 15 seconds.
196 Lower detection limits for the observed VOCs are estimated to be 20 ppt for a 5 second
197 integration with sensitivity of 70 counts ppb^{-1} (2 σ). The uncertainty is estimated as 12 %
198 (2 σ) for the same integration time. Meteorological parameters such as temperature and
199 humidity are monitored by LSI LASTEM Meteorological Sensors. All the presented data
200 is from the 15 m (the canopy height is 18 m) sampling line and meteorological sensors
201 collocated at this height too.
202 PTR-MS with a quadrupole mass filter has an intrinsic limitation that isobaric
203 compounds are all collectively quantified with the same channel (m/z) with a resolution
204 of unit mass. This limitation particularly becomes an issue for investigating the roles of
205 different isomers of MT and sesquiterpenes (SQTs) in photochemistry. For this reason,
206 we also occasionally collect sorbent cartridge samples to analyze MT and SQT speciation
207 in both ambient air and branch enclosure emissions near the sampling tower. As
208 described in (Kim et al., 2013d), Tenax GR and Carbotrap 5TD packed sorbent cartridges
209 (Markes Int, Llanstrisant, UK) were used for sampling. The sampled cartridges were
210 shipped to National Center for Atmospheric Research (NCAR), Boulder CO, USA for
211 gas chromatography-mass spectrometer (GC-MS) analysis. An Agilent 7890 GC/5975 C
212 Electron Impact Mass Spectrometer (GC-MS/FID) in conjunction with a MARKES
213 Unity1/Ultra thermal desorption system optimized for terpenoid analysis quantifies
214 speciated MT and SQT in the sorbent samples. Cartridge samples are both collected from
215 ambient and branch enclosure air. Ambient samples were collected in the mid-day to
216 early afternoon with a volume of 6 L. Ozone in the ambient air was removed using a

217 Na_2SO_3 filter. Branch enclosure samples were also collected, mostly in the mid-day time
218 frame, with a volume of 1 L without an ozone filter as zero air was introduced to the
219 branch enclosure. To explore the diurnal differences in BVOC emissions, branch
220 enclosure samplings were conducted every two hours for three consecutive days in mid
221 June of 2013. We present these analytical results from GC-MS analysis limited to the
222 qualification purpose to examine MT and SQT speciation.
223
224 **2.2 HONO quantification**
225 HONO was measured with an ion chromatography (IC) coupled with diffusion
226 scrubber. Air was introduced to diffusion scrubber (Lab solutions Inc., IL, USA) through
227 a 2 m PFA tubing (1/4" i.d.) at 1.5 L m^{-1} using a filtered orifice restrictor (F-950, air
228 logic, WI, USA). Air flowing through diffusion scrubber interfaced with deionized water,
229 into which HONO was extracted. 50 μL of solution was injected into the IC system
230 through a PEEK loop (Rheodyne, WA, USA) and 6-way valve (EV750-100, Rheodyne,
231 WA, USA). Eluent was a mixture of Na_2CO_3 and $NaHCO_3$, which was pumped by a
232 HPLC pump (DX-100, Dionex, CA, USA) into a guard column (Ionpax® AG 14,
233 4x50mm, Dionex, CA, USA) and then analytical column (Ionpax® AS 14, 4x250mm,
234 Dionex, CA, USA). The column effluent passed through a suppressor (ASRS 300,
235 Dionex, CA, USA) and HONO was detected as nitrite ion in conductivity detector (550,
236 Alltech, IL, USA). The entire measurement processes of sampling, chemical analysis, and
237 data acquisition were controlled by a digital timer and data acquisition software
238 (DSchrom-n, DS science, Korea), by which we obtained two measurements every hour.
239 The system was calibrated using a NO_2^- standard solution (Kanto chemical Co., Inc.,

240 Tokyo, Japan) whenever reagents were replaced. The detection limit was 0.15 ppb
241 estimated from 3σ of the lowest working standard. Specific analytical characteristics are
242 described in Simon and Dasgupta (1995) and Takeuchi et al. (2004).
243
244 **2.3 UWCM box model**
245 UWCM 2.1 is an open source box model coded by MATLAB (MathWorks®).
246 The model platform can be downloaded from a website
247 (http://sites.google.com/site/wolfegm/code-archive). The box model is embedded its own
248 HO_X ($OH+RO_2$)-RO_X (peroxyradical and alkoxy radical)-NO_X coupling chemical
249 mechanism. UWCM utilizes Master Chemical Mechanism version 3.2 (MCM 3.2)
250 (Jenkins et al., 1997; Saunders et al., 2003) for near-explicit VOC photo-oxidation
251 schemes. A more detailed model description can be found in Wolfe and Thornton (2011).
252 To minimize uncertainty from the parameterizations of transport and emission, we
253 constrained relatively long-lived trace gases presented in Figure 1. This box modeling
254 technique has been commonly used for examination of OH levels that can be justified by
255 the short chemical lifetime of OH (Kim et al., 2014;Kim et al., 2013c;Mao et al.,
256 2012;Mao et al., 2010). Recently developed isoprene photo-oxidation mechanisms
257 shown in Archibald et al. (2010b) are also incorporated in the model. In addition, Kim et
258 al. (2013c) and Wolfe et al. (2013) applied the model in the identical fashion as used for
259 this study to probe radical distributions using comprehensive observational datasets. This
260 study used the UWCM to simulate the diurnal variations of radical pool ($OH+HO_2+RO_2$)
261 distributions as observational parameters such as CO, NO_X, ozone, and VOCs are
262 constrained. To fully account for roles of OVOCs in the box model as radical sources, we

simulated three consecutive days and presented diurnal variations from the third day. The specific parameters (CO, NO_X, ozone, HONO and VOCs), constrained by observations are described in section 2.1 and 2.2 and presented in Figure 1.

3. Results and Discussion

3.1. Observational Results

Diurnal averages of observed trace gases (June 1st 2013 to June 6th 2013) are shown in Figure 1. The TRF observatory is in continuous operation and we choose this six day period because a regional high-pressure system caused a stagnant air pollution event in this period. In the center of Seoul (the real- time data available at http://www.airkorea.or.kr), carbon monoxide was observed in the similar levels during the focused period (June 1st to June 6th, 2013). On the other hand, the NO_2 level observed in central Seoul was much higher (20-50 ppb) compared with observed levels at TRF. The reason can be attributed to differences between the chemical lifetime of CO (~a month) and NO_2 (~a few hours to a day). The observations clearly indicate that the TRF is not directly influenced by fresh SMA pollution plumes although the TRF is very close to the center of Seoul (30 km away from the city center) as a regional modeling study shows most of CO and NO_X sources are located in the city center (Ryu et al., 2013). Similar observations were also reported for other East Asian megacities such as Beijing (Ma et al., 2012), where ~ 30 ppb and ~ 15 ppb of NO_2 were observed at noon in the urban and the adjacent rural sites, respectively. In contrast, there were no noticeable differences in CO levels between the urban and rural sites (~ 1-2 ppm). The observed CO, NO_X and SO_2 levels in TRF were much lower than those observed in the suburban

Saewung Kim 3/25/2015 1:53 PM
Deleted: 2

Saewung Kim 3/25/2015 1:53 PM
Deleted: 2

Saewung Kim 3/25/2015 1:53 PM
Deleted: 2

289 regions of Chinese megacities such as Beijing (Ma et al., 2012), Shanghai (Tie et al.,
290 2013), and the Pearl River Delta Region (Lu et al., 2012) and similar with the observed
291 levels in Tokyo, Japan (Yoshino et al., 2012).
292 Previous VOC observations in the SMA consistently have shown that toluene is
293 the dominant anthropogenic VOC followed by other aromatic compounds such as xylene
294 and benzene (Kim et al., 2012;Na and Kim, 2001). Na and Kim (2001) reported high
295 concentrations of propane from house hold fuel use. However, recent observation results
296 from the photochemical pollution observational network managed by National Institute of
297 Environmental Research (NIER) of South Korea in the SMA clearly indicate that propane
298 levels have declined and are now much lower than the levels previously observed (NIER,
299 2010). This is probably caused by the implementation of a policy changing household
300 fuel sources from propane to methane. Kim et al. (2012) presented detailed aromatic
301 VOC distributions in the SMA from four different urban observational sites. In average,
302 toluene concentrations were observed ~ 7 times higher than the observed levels of xylene
303 and benzene. At the TRF, a similar anthropogenic VOC speciation distribution was
304 observed as shown in Figure 1. The observed toluene and MEK (methyl ethyl ketone)
305 mixing-ratios were much higher than benzene and xylene. MEK is detected in m/z of 73^+
306 by PTR-MS. Although methyl glyoxal, an atmospheric VOC oxidation product, is also
307 detected on the same mass, we assumed that 73^+ of m/z signals are mostly from MEK, an
308 anthropogenic VOC, since the temporal variation follows that of anthropogenic VOC
309 such as toluene and xylene. In addition, atmospheric lifetime of methyl glyoxal is much
310 shorter than MEK.

As the observation facility is located in the middle of a pine tree plantation (*Pinus koraiensis*), monoterpenes (MT) are consistently observed. The temporal variation of monoterpenes is affected by the planetary boundary layer evolution with a pattern of higher MT levels during night than those of mid-day as has been often reported in other forest environments (Bryan et al., 2012;Kim et al., 2010) This can be explained by interplays between boundary layer evolution and temperature dependent MT emission. It should also be noted that the continuous branch enclosure BVOC emission observations indicate that the daily maxima of MT and SQT emissions were observed in the midday (between noon to 2 pm in the local time). The observed MT and SQT speciation information in the midday is summarized in Table 2. Table 2a summarizes branch enclosure sample analysis results and ambient sample analysis results are summarized in Table 2b. In general, observed MT and SQT in the ambient air are consistent with previously observed distributions (Kim et al., 2013d). α-pinene and β-pinene were the dominant monoterpene and longifolene was the only detected SQT species. In contrast, the branch enclosure observation results, reflecting BVOC emission, indicate high emission of very reactive MT and SQT species such as β-myrcene, α-caryophyllene, and β-caryophyllene. The fast oxidation of these highly reactive terpenoid species is expected to limit the atmospheric presence of the compounds. Therefore, photochemical oxidation processes of these compounds may have been neglected. Investigating emissions and photochemistry of these reactive terpenoid compounds can constrain potential missing OH reactivity and SOA production from highly oxidized reaction products.

Isoprene is produced from carbon recently fixed through photosynthesis resulting in higher emissions and atmospheric concentrations during the daytime. The temporal

variation shown in Figure 1 reveals an isoprene concentration maximum between 17:00 to 20:00. In addition, the ratios of MVK+MACR, major isoprene oxidation products and isoprene at this period, are significantly lower than those of late morning to early afternoon. The enhanced isoprene levels in the late afternoon or early evening have been also reported in previous studies (Apel et al., 2002;Bryan et al., 2012). The branch enclosure observations demonstrate that isoprene is not emitted from the pine plantation but rather transported from surrounding broadleaf forests as right outside of the pine plantation (200 m × 200 m) is a forested area dominated by oak trees. Oak comprises 85 % of broadleaf trees in South Korea (Lim et al., 2011). Lim et al. (2011) quantified isoprene emission rates for five representative oak species in South Korea and report a wide emission range from oaks that are negligible isoprene emitters (<0.004 μgC dw^{-1} h^{-1}; standard emission rates) to others with very high isoprene emission rates of 130 μgC dw^{-1} h^{-1}. It is also noticeable that isoprene is observed in high levels (up to 1 ppb) even during the night. Observational results from the Pearl River Delta region in China also show high isoprene concentration episodes of more than 1 ppb during the night (Lu et al., 2012). As there are some speculations on potential artifacts on isoprene measurements using PTR-MS in environments with large oil and gas evaporative sources (Yuan et al., 2014), the assessments of the potential artifacts should be investigated further in the Asian megacity region.

Contributions from each trace gas species towards ambient OH reactivity are shown in Figure 2. This is calculated as the product of the observed species concentration and its rate constant for reaction with OH. Observed OH reactivity from VOCs are much higher than from other trace gases such as CO, NOx, SO_2, and ozone. Among the

observed VOC species, BVOCs such as isoprene, α-pinene and β-pinene accounted for significantly higher OH reactivity in comparison with the observed AVOCs such as toluene, benzene, xylene and MEK. Isoprene accounts the highest OH reactivity especially during the daytime. This analysis is consistent with reports from other suburban observations from East Asian megacities such as Beijing (Ran et al., 2011), the PRD region, China (Lou et al., 2010), and the Kinki region Japan (Bao et al., 2010).

HONO levels up to 1 ppb were observed in the early morning and were consistently higher than 0.5 ppb during the daytime. These observed levels are substantially higher than reported observations from forest environments in North America (Ren et al., 2011;Zhou et al., 2011), where NO_X (~ 1 ppb) is substantially lower than the level observed at TRF. Ren et al. (2011) reported 30 – 60 ppt of HONO at the Blodgett Forest Research Station in the western foothills of the Sierra Nevada Mountains in the late summer of 2007. Zhou et al. (2011) also reported the similar levels of HONO (below 100 ppt) from the PROPHET forest, a mixed hardwood forest in northern Michigan (Pellston, MI). However, significantly higher HONO levels (~ 200 ppt to ~ 2 ppb) were reported by Li et al. (2012) from a rural observational site in the Pearl River Delta region near Guangzhou, where comparable NO_2 levels with TRF were observed. The high HONO levels (a few hundred ppt) especially during the daytime have been consistently reported near Eastern Asian megacities such as Beijing (Li et al., 2012), Shanghai (Hao et al., 2006), and Seoul (Song et al., 2009). Still these are limited datasets and further comprehensive analysis, especially more extensive observation is required. However, recently proposed HONO production mechanisms may be able to explain the higher levels in the Eastern Asian megacity region. One is HONO production from NO_2

Saewung Kim 3/25/2015 9:41 AM
Deleted: two

photo-excitation (Wong et al., 2012) as the region usually has high NO_2 concentrations. Zhou et al. (2011) claimed that significant HONO could be generated from nitrate photolysis processes on forest canopy surface by presenting observational data from a hardwood forest in Pellston, MI. Finally, HONO emission from soil bacteria is also proposed (Oswald et al., 2013). Oswald et al. (2013) found differences as much as two orders of magnitude in HONO emissions from soil samples from different environments (e.g. pH and nutrient contents). In addition, as most of observations in the East Asia regions were conducted with ion chromatography based methods, more direct HONO quantification techniques such as a chemical ionization mass spectrometry technique (Roberts et al., 2010) need to be used to characterize any potential interferences such a high NO_X environment (e.g. N_2O_5).

Saewung Kim 3/25/2015 9:57 AM
Deleted: and

Saewung Kim 3/25/2015 9:44 AM
Deleted: the other is HONO emission from soil bacteria (Oswald et al., 2013).

3.2 HO_X Model calculations to examine different isoprene photo-oxidation scenarios and the roles of unconstrained HONO sources.

The presented observational results are used to constrain the UWCM box model. We evaluate uncertainties in the tropospheric oxidation capacity and how it affects our ability to constrain ozone and OVOCs production. The observational results clearly indicate that isoprene is the most dominant OH sink among the observed VOCs. In addition, NO concentrations were higher in the 600 to 800 ppt range in the morning. On the other hand, afternoon levels were substantially lower in the 50 to 100 ppt range. The environment provides a unique opportunity to examine implications of isoprene photochemistry in various NO conditions.

406 We conducted model simulation under four different scenarios. Each scenario is
407 described in Table 3. The quantitative assessments of the impacts on radical
408 concentrations (OH, HO_2, and RO_2) from unknown HONO sources are evaluated by
409 examining the outcomes of the model simulations with and without observed HONO. To
410 evaluate the impacts of hydroperoxy-methyl-butenal (HPALD) photolysis and isoprene
411 peroxy radical recycling in the radical pool, each chemical mechanism is selectively
412 constrained by different scenarios. For HPALD chemistry, we adapted two different
413 HPALD formation rate constants published by Peeters and Muller (2010) and Crounse et
414 al. (2011). The formation rates from Peeters and Muller (2010) are about 40 times faster
415 than those from Crounse et al. (2011) in 298 K. Although there have been speculations
416 about other radical recycling mechanisms such as peroxy radical-peroxy radical reactions
417 (Lelieveld et al., 2008) and unknown reducing agents showing similar chemical
418 behaviors as NO (Hofzumahaus et al., 2009), we do not evaluate these possibilities as
419 there are no specific chemical mechanisms.
420 Modeled OH, HO_2, and RO_2 from the four different model scenarios are shown in
421 Figure 3. A summary of averaged OH, HO_2, and RO_2 concentrations in the morning
422 (08:00 – 11:00) and the afternoon (13:00 – 16:00) from each simulation is shown in
423 Table 4. With respect to the base run results (Scenario I), Scenario III with the lower
424 HPALD formation rate does not cause noticeable differences in radical concentrations.
425 Adapting higher HPALD formation rates (Scenario II) cause significant differences in
426 radical distribution especially in RO_2. This difference is likely caused by the fact that
427 significant isoprene peroxy radical is converted to HPALD. The higher levels of
428 discrepancy is found in RO_2 between Scenario I and Scenario II in the afternoon when

Saewung Kim 3/25/2015 10:09 AM
Deleted: to

Saewung Kim 3/25/2015 10:05 AM
Deleted: is

Saewung Kim 3/26/2015 8:27 AM
Deleted: six

low NO concentrations are observed, which efficiently facilitates HPALD formation. Similarly, a larger OH discrepancy (~ 20 %) between Scenario I and Scenario II is observed in the afternoon.

Striking differences can be found in the model simulation results with or without constraining observed HONO as shown in Figure 3. Model calculation results from Scenario IV indicate significantly smaller OH, HO_2, and RO_2 concentrations than the concentrations calculated from the counter part (Scenario I), which contains identical constraints and isoprene photochemistry except constraining observed HONO. Again, this clearly indicates that more thorough evaluations of the impacts of HONO on air quality are needed to precisely constrain photochemical processes in the region along with evaluations of the currently available analytical techniques as argued in section 3.1.

3.3 Implications of the uncertainty in HO_X estimations in assessing photochemical ozone and OVOC production.

Two competing chemical reactions (R3 vs. R4,5,6) determine radical distribution regimes.

$$RO_2 + NO \rightarrow RO + NO_2 \quad (R3)$$

$$RO_2 + HO_2 \rightarrow ROOH + O_2 \quad (R4)$$

$$RO_2 + RO_2 \rightarrow ROOR + O_2 \quad (R5)$$

$$HO_2 + HO_2 \rightarrow H_2O_2 + O_2 \quad (R6)$$

When the rate of R3 gets much faster than the sum of reaction rates of R4, R5, and R6 then radical recycling processes become more efficient than radical destruction

processes. In this radical recycling regime, OH, a universal tropospheric oxidant, is well buffered to maintain the elevated OH levels. On the other hand, the radical destruction regime can be defined when the radical recycling rates (R3) are slower than the radical destruction reaction rates (R4+R5+R6). Although some recent field studies (e.g. Lelieveld et al. (2008)) suggest that we may need to reconsider R4 as a radical recycling process rather than a radical destruction process, in this study, we follow the conventional classification of radical chemistry regimes since recent laboratory characterizations have shown that OH recycling from the RO_2+HO_2 reaction should be insignificant (Liu et al., 2013;Villena et al., 2012;Fuchs et al., 2013) . The temporal variations of radical-radical reaction rates from the model simulation scenarios are shown in Figure 4. In general, the radical reaction rates are elevated as much as twice once observed HONO is constrained in the model calculations (e.g. Scenario IV). This is because unaccounted HONO in the model calculations cause significant underestimations in the radical pool ($OH+HO_2+RO_2$) size with respect to the constrained HONO scenarios as shown in Figure 4. In addition, in the afternoon when NO concentration becomes lower, the RO_2 + HO_2 reaction rates get close or slightly higher than those of RO_2 + NO in the afternoon for the all model scenarios, constrained by observed HONO. This is surprising, as the radical destruction regime is usually associated with low NO_X conditions. Suburban regions of megacities including the TRF in general show high NO_X conditions. However, radical recycling rates are determined by concentrations of NO. The fraction of NO in the NO_X pool is determined by competing reactions between NO_2 photolysis and oxidation reactions of NO by ozone, HO_2, and RO_2 radicals. Once we assume the pseudo-steady state of NO, then NO in NO_X pool (Leighton, 1961) can be expressed as

Saewung Kim 3/26/2015 8:58 AM
Deleted: as we include recently developed isoprene radical chemistry, the RO_2+HO_2 reaction rates, known for a radical destruction pathway becomes higher. This becomes more obvious i

Saewung Kim 3/26/2015 8:58 AM
Deleted: . Especially, in the case of Scenario II,

$$[NO] = J_{NO2}[NO_2]/(k_{NO+O3}[O_3] + k_{NO+HO2}[HO_2] + k_{NO+RO2}[RO_2]) \text{ (Eq 1)}$$

This mathematical expression clearly shows that NO levels are dependent on NO_X mostly composed of NO_2. At the same time, the fraction of NO in NO_X is anti-correlated with ozone, HO_2, and RO_2 concentrations. Therefore, the size of the radical pool composed of HO_2 and RO_2 is relevant for determining the fractions of NO in given NO_X levels. High HO_2 and RO_2 are likely observed in high VOC regions such as forested areas. This could cause a smaller fraction of NO in the given NO_X pool so radical recycling gets relatively weaker compared with radical destruction reaction pathways. More quantitative approaches are required to categorize radical reaction pathways rather than qualitative categorization such as high or low NO_X regimes. One should keep in mind that the pseudo-steady state assumption requires precise NO_2 quantification, which may not be the case in our study as the Mo-converter used for the NO_2 quantification could have interferences (Table 1). The overestimation due to thermal dissociations of reactive oxygenated nitrogen species has been reported to be 20 % to 83 % (Ge et al., 2013;Steinbacher et al., 2007). In addition, Mannschreck et al. (2004) presented the NO-NO_2-ozone photostationary state analysis using a four year dataset from a rural observational site in Hohenpeissenberg, Germany. The results indicate that the pseudo steady state assumption considering only NO-NO_2-ozone deviates about a factor of two from the stationary state on average. Even with the consideration of peroxy radical chemistry the pseudo steady state assumption is only valid for 13-32 % of the observational period. The authors speculated that local NO_2 sources, local NO or ozone

508 sinks, or rapid changes in J_{NO2} and ozone can break the pseudo-steady state. Nonetheless,
509 the argument that NO is a more critical parameter in determining radical distributions
510 than NO_X levels still holds.
511 Conventionally, efficient ozone production can be achieved by the balance
512 between nitric acid production rates (P_{HNO3}, $OH + NO_2$) and peroxide production rates
513 (P_{ROOH}, HO_2+RO_2 or P_{H2O2} HO_2+HO_2) (Sillman and He, 2002). The imbalance will cause
514 ozone production sensitivity towards either NOx or VOCs. A comprehensive
515 photochemical model analysis (Tonnesen and Dennis, 2000a, b) demonstrated that in a
516 wider range of ozone concentrations, the VOC and NOx limited regimes can be
517 determined by the ratios of P_{H2O2} and P_{HNO3}. Kleinman (2000) and Sillman and He (2002)
518 presented an observation-based ozone production regime evaluation method comparing
519 peroxide production rates (P(peroxide)) and nitric acid production rates ($P(HNO_3)$). This
520 categorization has guided policy-making processes whether NO_X or VOC controls will be
521 more effective in ozone reduction. A series of modeling studies have been conducted to
522 characterize ozone production regimes in the suburban regions of East Asian megacities
523 and have consistently concluded that the role of isoprene is important in ozone
524 production. However, most of these studies have concluded that East Asian megacity
525 regions are mostly in the VOC limited regime (Tseng et al., 2009;Zhang et al.,
526 2008b;Lim et al., 2011;Cheng et al., 2010;Shao et al., 2009a;Shao et al., 2009b;Xing et
527 al., 2011). Recently, however, a modeling study by Li et al. (2013) in the Pearl River
528 Delta region in China demonstrated the time dependence of ozone production regimes.
529 Specifically, with high NOx emissions in the morning, the regional ozone production
530 regime is categorized as VOC limited. In contrast, in the afternoon when the highest

ozone concentrations are observed, a NOx limited regime is often found. In addition, a box modeling study constrained by observation on top of Mt. Tai in Central East China also reported NO_X limited ozone production regime (Kanaya et al., 2009). The obvious issue to be addressed is that all of the above studies neglected how the uncertainty in hydroxyl radical chemistry would affect the ozone production regime. Moreover, HONO has been rarely constrained by observations in the previous modeling studies. Figure 5 shows the temporal variations of 2 P(peroxide)/P(HNO_3) from all four different model scenarios. As shown in the figure, the ratio above 1 indicates the NO_X limited regime and the VOC limited regime can be determined when the ratio is below 1. The NO_X limited ozone formation regime occurred on most days except the morning when high NO_X levels were observed regardless of the HO_X simulation scenarios. This is consistent with the recent modeling study for the Pearl River Delta region by Li et al. (2013). Differences among the scenarios are not noticeable in the morning when NO is high but noticeable differences can be found in the afternoon which may cause uncertainty in assessing the optimal level of NO_X and VOC emission controls from a policy perspective. In general, the model calculation results with faster HPALD formation rates indicate lower 2P(peroxide)/P(HNO_3) in the afternoon. This analysis indicates that it is difficult to determine an effective policy implementation for NO_X or VOC controls to achieve ozone abatement around Asian megaticities where isoprene is a significant OH sink without accurate understanding of radical-isoprene interactions (e.g. Kim et al. (2013b)). Again, it should be noted the possibility of systematic NO_2 overestimations from the Mo-converter use as discussed. The overestimation will directly translate into overestimated P(HNO_3).

Saewung Kim 3/26/2015 4:30 PM
Formatted: Subscript

Saewung Kim 3/26/2015 10:14 AM
Formatted: Subscript

Saewung Kim 3/26/2015 10:21 AM
Formatted: Subscript

Therefore, it is likely that the ozone production regime at TRF is shifted towards the NO_X limited regime in reality.

Saewung Kim 3/26/2015 10:21 AM
Formatted: Subscript

Another unresolved uncertainty in understanding tropospheric OH is its chemical loss rates. The limited observations of OH reactivity in BVOC dominant environments show consistent unaccounted OH chemical loss with observational datasets (Di Carlo et al., 2004;Edwards et al., 2013;Kim et al., 2011;Lou et al., 2010;Nolscher et al., 2012;Nakashima et al., 2014;Sinha et al., 2010). Two different processes are speculated to cause unaccounted OH loss known as missing OH reactivity: 1) primary emissions of unmeasured or unknown compounds and 2) oxidation products of well-known BVOCs especially isoprene. Most studies conducted in coniferous forests where monoterpenes are dominant primary BVOC emissions have concluded that unmeasured or unknown primary BVOC emissions caused missing OH reactivity (Sinha et al., 2010;Nakashima et al., 2014). On the other hand, studies conducted in isoprene dominant environments in mostly broadleaf or mixed forests have concluded that the main cause of missing OH reactivity is the oxidation products of isoprene (Edwards et al., 2013;Kim et al., 2011). Edwards et al. (2013) presented a thorough analysis on potential impacts of isoprene oxidation products that are not routinely constrained by observations. The authors found significant contributions from secondary oxidation products such as multi-functional oxygenated compounds.

Figure 6a shows the temporal variations of total OH reactivity calculated from five different model scenarios (I through IV). The highest and the lowest OH reactivity levels were predicted from model calculations of Scenario I and Scenario IV, respectively. This observation is directly correlated with calculated RO_2 levels as the lowest and

highest RO_2 levels were calculated from Scenario I and Scenario IV, respectively. Since VOC precursors and trace gases were all constrained by observations in the model calculations, the differences in model calculated OH reactivity should be mainly caused by the oxidation products of VOCs. This can be confirmed by the comparisons of model calculated formaldehyde concentrations from Scenario I and IV as formaldehyde is a dominant oxidation product of isoprene (Figure 6b). The differences in formaldehyde levels suggest differences in OH reactivity levels from OVOCs in each model simulation. In summary, uncertainty in radical distributions especially RO_2 levels is directly propagated into uncertainty in OVOC formation.

These calculated results provide an upper limit of potential contributions from the oxidation products of the constrained VOC precursors considering that the box-model does not consider dry-deposition processes as Karl et al. (2010) and Edwards et al. (2013) suggested that there is significant uncertainty associated with the parameterizations of dry deposition especially OVOCs. Still, this analysis suggests that significant missing OH reactivity can be found without constraining OVOCs. OVOCs, especially multi-functional highly oxidized compounds are precursors for secondary organic aerosols (SOA). Therefore, uncertainty surrounding missing OH reactivity significantly undermines our ability to constrain SOA formation and aerosol growth.

Saewung Kim 3/26/2015 10:01 AM
Deleted: (~ up to factor of two to three)

Saewung Kim 3/26/2015 10:01 AM
Deleted: VOCs

4. Summary and conclusions

We presented trace gas observation results from the TRF near the center of Seoul, South Korea. The dataset provides important constraints to evaluate the HO_X pool at the site where both anthropogenic and biogenic influences become important factors in

601 determining oxidation capacity. Although the site is in the vicinity of a megacity with 25
602 million people, isoprene accounted for most of the OH loss from observed atmospheric
603 hydrocarbon species during the 6-day focus period in early June 2013 during a regional
604 pollution episode. In addition, observed NO_X levels were substantially lower than
605 observed values in the center of the SMA. These observations indicate that impacts of
606 megacity pollution on suburban BVOC photochemistry can be observed at the TRF.
607 Four different model scenarios are employed to investigate the radical (OH, HO_2,
608 and RO_2) distributions using the UWCM box-model. The observed trace gas data were
609 constrained and the photochemical mechanisms (MCM 3.2) of seven VOC species with
610 high levels at the TRF were integrated. The uncertainty in isoprene peroxy radical
611 chemistry results in a wider range of OH, HO_2, and RO_2 distributions. Unconstrained
612 HONO sources also cause a quite high level of underestimation in a radical pool
613 ($OH+HO_2+RO_2$). OH simulation from the different model scenarios indicates much
614 larger discrepancies (up to three times) than simulations for HO_2 and RO_2 (up to twofold).
615 OH is simulated in higher levels with the consideration of an additional OH recycling
616 channel from fast HPALD formation chemistry Peeters and Muller (2010). On the other
617 hand, the RO_2 simulations result in lower levels as HPALD formation depletes the RO_2
618 pool, which mostly composed by isoprene peroxy radicals. These results suggest that
619 direct HO_2 and RO_2 observations can provide pivotal information about radical recycling
620 and isoprene peroxy radical chemistry (Kim et al., 2013c;Wolfe et al., 2013). More
621 studies on characterizing existing techniques to quantify HO_2 (Fuchs et al., 2011) and
622 developing new techniques (Horstjann et al., 2013) are needed. In addition, the
623 simulations with recently developed isoprene photo-oxidation chemistry show that

Saewung Kim 3/25/2015 1:53 PM
Deleted: 2

625 radical termination processes (e.g. peroxide formation) get more efficient than radical
626 recycling processes in the afternoon. This may come as a surprise as in general we expect
627 the high NO_X conditions in the suburban regions of a megacity to have effective radical
628 recycling. However, the critical factor determining competing reaction channels of
629 recycling and peroxide formation is NO concentrations. Ratios of NO to NO_2 are not only
630 correlated with NO_2 concentrations and photolysis constants but also anti-correlated with
631 RO_2, HO_2 and ozone concentrations and relevant kinetic constants as shown in (Eq 1).
632 Therefore, a semi-quantitative term such as the high 'NO_X' regime is not a proper term to
633 define radical recycle regimes especially in high radical environments (e.g. HO_2 and RO_2)
634 such as forest environments.
635 These uncertainties in estimating the radical pool size and distribution directly
636 affect our ability for constraining photochemical ozone and OVOC production. The non-
637 linear response of ozone production to NO_X and VOC abundances are determined by OH,
638 HO_2, RO_2 and NO_2 concentrations. Regardless of which model calculation scenario we
639 adapt, the TRF photochemical state appears to be a NO_X limited ozone production regime,
640 except for the morning when the VOC limited regime is observed. A noticeable range of
641 NO_X sensitivity was calculated from the four different model scenarios, especially in the
642 afternoon. These analysis results, therefore, suggest that an accurate scientific
643 understanding of isoprene-OH interactions should form the basis for an effective policy
644 implementation to reduce photochemical pollution in the suburbs of Seoul and similar
645 East Asian megacities. In addition, OVOC production is predicted to significantly vary
646 depending on the model simulation scenarios. The fate of these OVOCs is uncertain and
647 can include deposition, photolysis, or condensation. Our limited understanding of

OVOCs contributes substantially to the overall uncertainty in radical photochemistry and should be addressed by studies that quantify the processes controlling OVOC production and loss.

Acknowledgements

This research is financially supported by the National Institute of Environmental Research of South Korea. The authors appreciate logistical support from the research and supporting staff at Taehwa Research Forest operated by Seoul National University.

References

Apel, E. C., Riemer, D. D., Hills, A., Baugh, W., Orlando, J., Faloona, I., Tan, D., Brune, W., Lamb, B., Westberg, H., Carroll, M. A., Thornberry, T., and Geron, C. D.: Measurement and interpretation of isoprene fluxes and isoprene, methacrolein, and methyl vinyl ketone mixing ratios at the PROPHET site during the 1998 Intensive, J Geophys Res-Atmos, 107, Artn 4034
Doi 10.1029/2000jd000225, 2002.

Archibald, A. T., Cooke, M. C., Utembe, S. R., Shallcross, D. E., Derwent, R. G., and Jenkin, M. E.: Impacts of mechanistic changes on HOx formation and recycling in the oxidation of isoprene, Atmos Chem Phys, 10, 8097-8118, Doi 10.5194/Acp-10-8097-2010, 2010a.

Archibald, A. T., Jenkin, M. E., and Shallcross, D. E.: An isoprene mechanism intercomparison, Atmos Environ, 44, 5356-5364, Doi 10.1016/J.Atmosenv.2009.09.016, 2010b.

Arneth, A., Schurgers, G., Lathiere, J., Duhl, T., Beerling, D. J., Hewitt, C. N., Martin, M., and Guenther, A.: Global terrestrial isoprene emission models: sensitivity to variability in climate and vegetation, Atmos Chem Phys, 11, 8037-8052, Doi 10.5194/Acp-11-8037-2011, 2011.

Bao, H., Shrestha, K. L., Kondo, A., Kaga, A., and Inoue, Y.: Modeling the influence of biogenic volatile organic compound emissions on ozone concentration during summer season in the Kinki region of Japan, Atmos Environ, 44, 421-431, Doi 10.1016/J.Atmosenv.2009.10.021, 2010.

Barket, D. J., Hurst, J. M., Couch, T. L., Colorado, A., Shepson, P. B., Riemer, D. D., Hills, A. J., Apel, E. C., Hafer, R., Lamb, B. K., Westberg, H. H., Farmer, C. T., Stabenau, E. R., and Zika, R. G.: Intercomparison of automated methodologies for determination of ambient isoprene during the PROPHET 1998 summer campaign, J Geophys Res-Atmos, 106, 24301-24313, Doi 10.1029/2000jd900562, 2001.

Saewung Kim 3/26/2015 4:36 PM
Formatted: Indent: Left: 0", Hanging: 0.38", Tabs: 0.13", Left

Saewung Kim 3/26/2015 4:36 PM
Formatted: Font:(Default) Times New Roman

Blake, R. S., Monks, P. S., and Ellis, A. M.: Proton-Transfer Reaction Mass Spectrometry, Chem Rev, 109, 861-896, 2009.

Bryan, A. M., Bertman, S. B., Carroll, M. A., Dusanter, S., Edwards, G. D., Forkel, R., Griffith, S., Guenther, A. B., Hansen, R. F., Helmig, D., Jobson, B. T., Keutsch, F. N., Lefer, B. L., Pressley, S. N., Shepson, P. B., Stevens, P. S., and Steiner, A. L.: In-canopy gas-phase chemistry during CABINEX 2009: sensitivity of a 1-D canopy model to vertical mixing and isoprene chemistry, Atmos Chem Phys, 12, 8829-8849, Doi 10.5194/Acp-12-8829-2012, 2012.

Chameides, W. L., Lindsay, R. W., Richardson, J., and Kiang, C. S.: The Role of Biogenic Hydrocarbons in Urban Photochemical Smog - Atlanta as a Case-Study, Science, 241, 1473-1475, 1988.

Chang, C. C., Wang, J. L., Leung, S.-C. C., Chang, C. Y., Lee, P.-J., Chew, C., Liao, W.-N., and Ou-Yang, C.-F.: Seosonal characteristics of biogenic and anthropogenic isoprene in tropical-subtropical urban environments, Atmos Environ, 99, 298-308, 2014.

Cheng, H. R., Guo, H., Saunders, S. M., Lam, S. H. M., Jiang, F., Wang, X. M., Simpson, I. J., Blake, D. R., Louie, P. K. K., and Wang, T. J.: Assessing photochemical ozone formation in the Pearl River Delta with a photochemical trajectory model, Atmos Environ, 44, 4199-4208, Doi 10.1016/J.Atmosenv.2010.07.019, 2010.

Crounse, J. D., Paulot, F., Kjaergaard, H. G., and Wennberg, P. O.: Peroxy radical isomerization in the oxidation of isoprene, Phys Chem Chem Phys, 13, 13607-13613, Doi 10.1039/C1cp21330j, 2011.

de Gouw, J., and Warneke, C.: Measurements of volatile organic compounds in the earths atmosphere using proton-transfer-reaction mass spectrometry, Mass Spectrom Rev, 26, 223-257, 2007.

Di Carlo, P., Brune, W. H., Martinez, M., Harder, H., Lesher, R., Ren, X. R., Thornberry, T., Carroll, M. A., Young, V., Shepson, P. B., Riemer, D., Apel, E., and Campbell, C.: Missing OH reactivity in a forest: Evidence for unknown reactive biogenic VOCs, Science, 304, 722-725, Doi 10.1126/Science.1094392, 2004.

Dreyfus, G. B., Schade, G. W., and Goldstein, A. H.: Observational constraints on the contribution of isoprene oxidation to ozone production on the western slope of the Sierra Nevada, California, J Geophys Res-Atmos, 107, Artn 4365
Doi 10.1029/2001jd001490, 2002.

Edwards, P. M., Evans, M. J., Furneaux, K. L., Hopkins, J., Ingham, T., Jones, C., Lee, J. D., Lewis, A. C., Moller, S. J., Stone, D., Whalley, L. K., and Heard, D. E.: OH reactivity in a South East Asian tropical rainforest during the Oxidant and Particle Photochemical Processes (OP3) project, Atmos Chem Phys, 13, 9497-9514, Doi 10.5194/Acp-13-9497-2013, 2013.

Fuchs, H., Bohn, B., Hofzumahaus, A., Holland, F., Lu, K. D., Nehr, S., Rohrer, F., and Wahner, A.: Detection of HO2 by laser-induced fluorescence: calibration and interferences from RO2 radicals, Atmos Meas Tech, 4, 1209-1225, Doi 10.5194/Amt-4-1209-2011, 2011.

Fuchs, H., Hofzumahaus, A., Rohrer, F., Bohn, B., Brauers, T., Dorn, H. P., Haseler, R., Holland, F., Kaminski, M., Li, X., Lu, K., Nehr, S., Tillmann, R., Wegener, R., and Wahner, A.: Experimental evidence for efficient hydroxyl radical regeneration in isoprene oxidation, Nat Geosci, 6, 1023-1026, Doi 10.1038/Ngeo1964, 2013.

Ge, B. Z., Sun, Y. L., Liu, Y., Dong, H. B., Ji, D. S., Jiang, Q., Li, J., and Wang, Z. F.: Nitrogen dioxide measurement by cavity attenuated phase shift spectroscopy (CAPS) and implications in ozone production efficiency and nitrate formation in Beijing, China, J Geophys Res-Atmos, 118, 9499-9509, Doi 10.1002/Jgrd.50757, 2013.

Guenther, A.: Biological and chemical diversity of biogenic volatile organic emissions into the atmosphere, Atmospheric Sciences, 2013, ArticleID 786290, 2013.

Hao, N., Zhou, B., Chen, D., and Chen, L. M.: Observations of nitrous acid and its relative humidity dependence in Shanghai, J Environ Sci-China, 18, 910-915, Doi 10.1016/S1001-0742(06)60013-2, 2006.

Hofzumahaus, A., Rohrer, F., Lu, K. D., Bohn, B., Brauers, T., Chang, C. C., Fuchs, H., Holland, F., Kita, K., Kondo, Y., Li, X., Lou, S. R., Shao, M., Zeng, L. M., Wahner, A., and Zhang, Y. H.: Amplified Trace Gas Removal in the Troposphere, Science, 324, 1702-1704, 10.1126/science.1164566, 2009.

Horstjann, M., Andres Hernandez, M. D., Nenakhov, V., Chrobry, A., and Burrows, J. P.: Peroxy radical detection for airborne atmospheric measurements using cavity ehnaced absorption spectroscopy of NO2, Atmospheric Measurement Techniques Discussion, 6, 9655-9688, 2013.

Huang, M., Bowman, K. W., Carmichael, G. R., Pierce, R. B., Worden, H. M., Luo, M., Cooper, O. R., Pollack, I. B., Ryerson, T. B., and Brown, S. S.: Impact of Southern California anthropogenic emissions on ozone pollution in the mountain states: Model analysis and observational evidence from space, J Geophys Res-Atmos, 118, 12784-12803, Doi 10.1002/2013jd020205, 2013.

Kanaya, Y., Pochanart, P., Liu, Y., Li, J., Tanimoto, H., Kato, S., Suthawaree, J., Inomata, S., Taketani, F., Okuzawa, K., Kawamura, K., Akimoto, H., and Wang, Z. F.: Rates and regimes of photochemical ozone production over Central East China in June 2006: a box model analysis using comprehensive measurements of ozone precursors, Atmos Chem Phys, 9, 7711-7723, 2009.

Karl, T., Harley, P., Emmons, L., Thornton, B., Guenther, A., Basu, C., Turnipseed, A., and Jardine, K.: Efficient Atmospheric Cleansing of Oxidized Organic Trace Gases by Vegetation, Science, 330, 816-819, Doi 10.1126/Science.1192534, 2010.

Kim, K. H., Ho, D. X., Park, C. G., Ma, C. J., Pandey, S. K., Lee, S. C., Jeong, H. J., and Lee, S. H.: Volatile Organic Compounds in Ambient Air at Four Residential Locations in Seoul, Korea, Environ Eng Sci, 29, 875-889, Doi 10.1089/Ees.2011.0280, 2012.

Kim, S., Karl, T., Guenther, A., Tyndall, G., Orlando, J., Harley, P., Rasmussen, R., and Apel, E.: Emissions and ambient distributions of Biogenic Volatile Organic Compounds (BVOC) in a ponderosa pine ecosystem: interpretation of PTR-MS mass spectra, Atmos Chem Phys, 10, 1759-1771, 2010.

Kim, S., Guenther, A., Karl, T., and Greenberg, J.: Contributions of primary and secondary biogenic VOC tototal OH reactivity during the CABINEX (Community Atmosphere-Biosphere INteractions Experiments)-09 field campaign, Atmos Chem Phys, 11, 8613-8623, 2011.

Kim, S., Guenther, A., and Apel, E.: Quantitative and qualitative sensing techniques for biogenic volatile organic compounds and their oxidation products, Environ Sci-Proc Imp, 15, 1301-1314, Doi 10.1039/C3em00040k, 2013a.

Kim, S., Lee, M., Kim, S., Choi, S., Seok, S., and Kim, S.: Photochemical characteristics of high and low ozone episodes observed in the Taehwa Forest observatory (TFO) in June 2011 near Seoul South Korea, Asia-Pacific Journal of Atmospheric Sciences, 49, 325-331, Doi 10.1007/S13143-013-0031-0, 2013b.

Kim, S., Wolfe, G. M., Mauldin, L., Cantrell, C., Guenther, A., Karl, T., Turnipseed, A., Greenberg, J., Hall, S. R., Ullmann, K., Apel, E., Hornbrook, R., Kajii, Y., Nakashima, Y., Keutsch, F. N., DiGangi, J. P., Henry, S. B., Kaser, L., Schnitzhofer, R., Graus, M., Hansel, A., Zheng, W., and Flocke, F. F.: Evaluation of HOx sources and cycling using measurement-constrained model calculations in a 2-methyl-3-butene-2-ol (MBO) and monoterpene (MT) dominated ecosystem, Atmos Chem Phys, 13, 2031-2044, Doi 10.5194/Acp-13-2031-2013, 2013c.

Kim, S., VandenBoer, T. C., Young, C. J., Riedel, T. P., Thornton, J. A., Swarthout, B., Sive, B., Lerner, B., Gilman, J. B., Warneke, C., Roberts, J. M., Guenther, A., Wagner, N. L., Dube, W. P., Williams, E., and Brown, S. S.: The primary and recycling sources of OH during the NACHTT-2011 campaign: HONO as an important OH primary source in the wintertime, J Geophys Res-Atmos, 119, 6886-6896, Doi 10.1002/2013jd019784, 2014.

Kim, S. Y., Jiang, X. Y., Lee, M., Turnipseed, A., Guenther, A., Kim, J. C., Lee, S. J., and Kim, S.: Impact of biogenic volatile organic compounds on ozone production at the Taehwa Research Forest near Seoul, South Korea, Atmos Environ, 70, 447-453, Doi 10.1016/J.Atmosenv.2012.11.005, 2013d.

Kleinman, L. I.: Ozone process insights from field experiments - part II: Observation-based analysis for ozone production, Atmos Environ, 34, 2023-2033, Doi 10.1016/S1352-2310(99)00457-4, 2000.

Leighton, P. A.: Photochemistry of Air Pollution, Academic, San Diego, CA USA, 1961.

Lelieveld, J., Butler, T. M., Crowley, J. N., Dillon, T. J., Fischer, H., Ganzeveld, L., Harder, H., Lawrence, M. G., Martinez, M., Taraborrelli, D., and Williams, J.: Atmospheric oxidation capacity sustained by a tropical forest, Nature, 452, 737-740, 2008.

Levy, H.: Normal Atmosphere - Large Radical and Formaldehyde Concentrations Predicted, Science, 173, 141-143, 1971.

Li, X., Brauers, T., Haseler, R., Bohn, B., Fuchs, H., Hofzumahaus, A., Holland, F., Lou, S., Lu, K. D., Rohrer, F., Hu, M., Zeng, L. M., Zhang, Y. H., Garland, R. M., Su, H., Nowak, A., Wiedensohler, A., Takegawa, N., Shao, M., and Wahner, A.: Exploring the atmospheric chemistry of nitrous acid (HONO) at a rural site in Southern China, Atmos Chem Phys, 12, 1497-1513, 2012.

Li, Y., Lau, A. K. H., Fung, J. C. H., Zheng, J. Y., and Liu, S. C.: Importance of NOx control for peak ozone reduction in the Pearl River Delta region, J Geophys Res-Atmos, 118, 9428-9443, Doi 10.1002/Jgrd.50659, 2013.

Lim, Y. J., Armendariz, A., Son, Y. S., and Kim, J. C.: Seasonal variations of isoprene emissions from five oak tree species in East Asia, Atmos Environ, 45, 2202-2210, Doi 10.1016/J.Atmosenv.2011.01.066, 2011.

Liu, Y. J., Herdlinger-Blatt, I., McKinney, K. A., and Martin, S. T.: Production of methyl vinyl ketone and methacrolein via the hydroperoxyl pathway of isoprene oxidation, Atmospheric Chemistry and Physics, 13, 5715-5730, Doi 10.5194/Acp-13-5715-2013, 2013.

Lou, S., Holland, F., Rohrer, F., Lu, K., Bohn, B., Brauers, T., Chang, C. C., Fuchs, H., Haseler, R., Kita, K., Kondo, Y., Li, X., Shao, M., Zeng, L., Wahner, A., Zhang, Y., Wang, W., and Hofzumahaus, A.: Atmospheric OH reactivities in the Pearl River Delta - China in summer 2006: measurement and model results, Atmos Chem Phys, 10, 11243-11260, 2010.

Lu, K. D., Rohrer, F., Holland, F., Fuchs, H., Bohn, B., Brauers, T., Chang, C. C., Haseler, R., Hu, M., Kita, K., Kondo, Y., Li, X., Lou, S. R., Nehr, S., Shao, M., Zeng, L. M., Wahner, A., Zhang, Y. H., and Hofzumahaus, A.: Observation and modelling of OH and HO2 concentrations in the Pearl River Delta 2006: a missing OH source in a VOC rich atmosphere, Atmos Chem Phys, 12, 1541-1569, Doi 10.5194/Acp-12-1541-2012, 2012.

Ma, J. Z., Wang, W., Chen, Y., Liu, H. J., Yan, P., Ding, G. A., Wang, M. L., Sun, J., and Lelieveld, J.: The IPAC-NC field campaign: a pollution and oxidization pool in the lower atmosphere over Huabei, China, Atmos Chem Phys, 12, 3883-3908, Doi 10.5194/Acp-12-3883-2012, 2012.

Mannschreck, K., Gilge, S., Plass-Duelmer, C., Fricke, W., and Berresheim, H.: Assessment of the applicability of NO-NO2-O-3 photostationary state to long-term measurements at the Hohenpeissenberg GAW Station, Germany, Atmos Chem Phys, 4, 1265-1277, 2004.

Mao, J., Ren, X., Zhang, L., Van Duin, D. M., Cohen, R. C., Park, J. H., Goldstein, A. H., Paulot, F., Beaver, M. R., Crounse, J. D., Wennberg, P. O., DiGangi, J. P., Henry, S. B., Keutsch, F. N., Park, C., Schade, G. W., Wolfe, G. M., Thornton, J. A., and Brune, W. H.: Insights into hydroxyl measurements and atmospheric oxidation in a California forest, Atmos Chem Phys, 12, 8009-8020, Doi 10.5194/Acp-12-8009-2012, 2012.

Mao, J. Q., Ren, X. R., Chen, S. A., Brune, W. H., Chen, Z., Martinez, M., Harder, H., Lefer, B., Rappengluck, B., Flynn, J., and Leuchner, M.: Atmospheric oxidation capacity in the summer of Houston 2006: Comparison with summer measurements in other metropolitan studies, Atmos Environ, 44, 4107-4115, Doi 10.1016/J.Atmosenv.2009.01.013, 2010.

Na, K., and Kim, Y. P.: Seasonal characteristics of ambient volatile organic compounds in Seoul, Korea, Atmos Environ, 35, 2603-2614, Doi 10.1016/S1352-2310(00)00464-7, 2001.

Nakashima, Y., Kato, S., Greenberg, J., Harley, P., Karl, T., Turnipseed, A., Apel, E., Guenther, A., Smith, J., and Kajii, Y.: Total OH reactivity measurements in ambient air in a southern Rocky mountain ponderosa pine forest during BEACHON-SRM08 summer campaign, Atmos Environ, 85, 1-8, Doi 10.1016/J.Atmosenv.2013.11.042, 2014.

NIER: Annual Report for Atmospheric Environment, National Insititute of Environmetal Rsearch, 2010.

Nolscher, A. C., Williams, J., Sinha, V., Custer, T., Song, W., Johnson, A. M., Axinte, R., Bozem, H., Fischer, H., Pouvesle, N., Phillips, G., Crowley, J. N., Rantala, P., Rinne, J., Kulmala, M., Gonzales, D., Valverde-Canossa, J., Vogel, A., Hoffmann, T., Ouwersloot, H. G., de Arellano, J. V. G., and Lelieveld, J.: Summertime total OH reactivity measurements from boreal forest during HUMPPA-COPEC 2010, Atmos Chem Phys, 12, 8257-8270, Doi 10.5194/Acp-12-8257-2012, 2012.

Oswald, R., Behrendt, T., Ermel, M., Wu, D., Su, H., Cheng, Y., Breuninger, C., Moravek, A., Mougin, E., Delon, C., Loubet, B., Pommerening-Roser, A., Sorgel, M., Poschl, U., Hoffmann, T., Andreae, M. O., Meixner, F. X., and Trebs, I.: HONO Emissions from Soil Bacteria as a Major Source of Atmospheric Reactive Nitrogen, Science, 341, 1233-1235, Doi 10.1126/Science.1242266, 2013.

Paulot, F., Crounse, J. D., Kjaergaard, H. G., Kroll, J. H., Seinfeld, J. H., and Wennberg, P. O.: Isoprene photooxidation: new insights into the production of acids and organic nitrates, Atmos Chem Phys, 9, 1479-1501, 2009.

Paulson, S. E., and Seinfeld, J. H.: Development and evaluation of a photooxidation mechanism for isoprene, Journal of Geophysical Research, 97, 20703-20715, 1992.

Peeters, J., and Muller, J. F.: HOx radical regeneration in isoprene oxidation via peroxy radical isomerisations. II: experimental evidence and global impact, Phys Chem Chem Phys, 12, 14227-14235, Doi 10.1039/C0cp00811g, 2010.

Pollack, I. B., Ryerson, T. B., Trainer, M., Neuman, J. A., Roberts, J. M., and Parrish, D. D.: Trends in ozone, its precursors, and related secondary oxidation products in Los Angeles, California: A synthesis of measurements from 1960 to 2010, J Geophys Res-Atmos, 118, 5893-5911, Doi 10.1002/Jgrd.50472, 2013.

Ran, L., Zhao, C. S., Xu, W. Y., Lu, X. Q., Han, M., Lin, W. L., Yan, P., Xu, X. B., Deng, Z. Z., Ma, N., Liu, P. F., Yu, J., Liang, W. D., and Chen, L. L.: VOC reactivity and its effect on ozone production during the HaChi summer campaign, Atmos Chem Phys, 11, 4657-4667, Doi 10.5194/Acp-11-4657-2011, 2011.

Ren, X., Sanders, J. E., Rajendran, A., Weber, R. J., Goldstein, A. H., Pusede, S. E., Browne, E. C., Min, K. E., and Cohen, R. C.: A relaxed eddy accumulation system for measuring vertical fluxes of nitrous acid, Atmos Meas Tech, 4, 2093-2103, Doi 10.5194/Amt-4-2093-2011, 2011.

Ryerson, T. B., Andrews, A. E., Angevine, W. M., Bates, T. S., Brock, C. A., Cairns, B., Cohen, R. C., Cooper, O. R., de Gouw, J. A., Fehsenfeld, F. C., Ferrare, R. A., Fischer, M. L., Flagan, R. C., Goldstein, A. H., Hair, J. W., Hardesty, R. M., Hostetler, C. A., Jimenez, J. L., Langford, A. O., McCauley, E., McKeen, S. A., Molina, L. T., Nenes, A., Oltmans, S. J., Parrish, D. D., Pederson, J. R., Pierce, R. B., Prather, K., Quinn, P. K., Seinfeld, J. H., Senff, C. J., Sorooshian, A., Stutz, J., Surratt, J. D., Trainer, M., Volkamer, R., Williams, E. J., and Wofsy, S. C.: The 2010 California Research at the Nexus of Air Quality and Climate Change (CalNex) field study, J Geophys Res-Atmos, 118, 5830-5866, Doi 10.1002/Jgrd.50331, 2013.

Ryu, Y. H., Baik, J. J., Kwak, K. H., Kim, S., and Moon, N.: Impacts of urban land-surface forcing on ozone air quality in the Seoul metropolitan area, Atmos Chem Phys, 13, 2177-2194, Doi 10.5194/Acp-13-2177-2013, 2013.

Sartelet, K. N., Couvidat, F., Seigneur, C., and Roustan, Y.: Impact of biogenic emissions on air quality over Europe and North America, Atmos Environ, 53, 131-141, Doi 10.1016/J.Atmosenv.2011.10.046, 2012.

Shao, M., Lu, S. H., Liu, Y., Xie, X., Chang, C. C., Huang, S., and Chen, Z. M.: Volatile organic compounds measured in summer in Beijing and their role in ground-level ozone formation, J Geophys Res-Atmos, 114, Artn D00g06
Doi 10.1029/2008jd010863, 2009a.

914 Shao, M., Zhang, Y. H., Zeng, L. M., Tang, X. Y., Zhang, J., Zhong, L. J., and Wang, B.
915 G.: Ground-level ozone in the Pearl River Delta and the roles of VOC and NO(x) in
916 its production, J Environ Manage, 90, 512-518, Doi
917 10.1016/J.Jenvman.2007.12.008, 2009b.
918 Sillman, S., and He, D.: Some theoretical results concerning O3-NOx-VOC chemistry
919 and NOx-VOC indicators, Journal of Geophysical Research, 107,
920 4659,doi:4610.1029:2001JD001123, 2002.
921 Sinha, V., Williams, J., Lelieveld, J., Ruuskanen, T. M., Kajos, M. K., Patokoski, J.,
922 Hellen, H., Hakola, H., Mogensen, D., Boy, M., Rinne, J., and Kulmala, M.: OH
923 Reactivity Measurements within a Boreal Forest: Evidence for Unknown Reactive
924 Emissions, Environ Sci Technol, 44, 6614-6620, Doi 10.1021/Es101780b, 2010.
925 Song, C. H., Park, M. E., Lee, E. J., Lee, J. H., Lee, B. K., Lee, D. S., Kim, J., Han, J. S.,
926 Moon, K. J., and Kondo, Y.: Possible particulate nitrite formation and its
927 atmospheric implications inferred from the observations in Seoul, Korea, Atmos
928 Environ, 43, 2168-2173, Doi 10.1016/J.Atmosenv.2009.01.018, 2009.
929 Spaulding, R. S., Schade, G. W., Goldstein, A. H., and Charles, M. J.: Characterization of
930 secondary atmospheric photooxidation products: Evidence for biogenic and
931 anthropogenic sources, J Geophys Res-Atmos, 108, Artn 4247
932 Doi 10.1029/2002jd002478, 2003.
933 Steinbacher, M., Zellweger, C., Schwarzenbach, B., Bugmann, S., Buchmann, B.,
934 Ordonez, C., Prevot, A. S. H., and Hueglin, C.: Nitrogen oxide measurements at
935 rural sites in Switzerland: Bias of conventional measurement techniques, J Geophys
936 Res-Atmos, 112, Artn D11307
937 Doi 10.1029/2006jd007971, 2007.
938 Tie, X., Geng, F., Guenther, A., Cao, J., Greenberg, J., Zhang, R., Apel, E., Li, G.,
939 Weinheimer, A., Chen, J., and Cai, C.: Megacity impacts on regional ozone
940 formation: observations and WRF-Chem modeling for the MIRAGE-Shanghai field
941 campaign, Atmos Chem Phys, 13, 5655-5669, Doi 10.5194/Acp-13-5655-2013,
942 2013.
943 Tonnesen, G. S., and Dennis, R. L.: Analysis of radical propagation efficiency to assess
944 ozone sensitivity to hydrocarbons and NOx 1. Local indicators of instantaneous odd
945 oxygen production sensitivity, J Geophys Res-Atmos, 105, 9213-9225, Doi
946 10.1029/1999jd900371, 2000a.
947 Tonnesen, G. S., and Dennis, R. L.: Analysis of radical propagation efficiency to assess
948 ozone sensitivity to hydrocarbons and NOx 2. Long-lived species as indicators of
949 ozone concentration sensitivity, J Geophys Res-Atmos, 105, 9227-9241, Doi
950 10.1029/1999jd900372, 2000b.
951 Trainer, M., Williams, E., Parrish, D. D., Buhr, M. P., Allwine, E. J., Westberg, H.,
952 Fehsenfeld, F. C., and Liu, S. C.: Models and observations of the impact of natural
953 hydrocarbons on rural ozone, Nature, 329, 705 - 707, 1987.
954 Tseng, K. H., Wang, J. L., Cheng, M. T., and Tsuang, B. J.: Assessing the Relationship
955 between Air Mass Age and Summer Ozone Episodes Based on Photochemical
956 Indices, Aerosol Air Qual Res, 9, 149-171, 2009.
957 VandenBoer, T., Murphy, J. G., Roberts, J. M., Middlebrook, A. M., Brock, C., Lerner,
958 B. M., Wolfe, D. E., Williams, E., Brown, S. S., Warneke, C., De Gouw, J.,
959 Wagner, N. L., Young, C. C., Dube, W. P., Bahreini, R., Riedel, T., Thornton, J. A.,

960 Ozturk, F., Keene, W., Maben, J. R., Pszenny, A., Kim, S., Grossberg, N., and
961 Lefer, B.: Understanding the role of the ground surface in HONO vertical structure:
962 High resolution vertical profiles during NACHTT-11, submitted, 2013.
963 Villena, G., Bejan, I., Kurtenbach, R., Wiesen, P., and Kleffmann, J.: Interferences of
964 commercial NO2 instruments in the urban atmosphere and in a smog chamber,
965 Atmos Meas Tech, 5, 149-159, Doi 10.5194/Amt-5-149-2012, 2012.
966 Wolfe, G. M., and Thornton, J. A.: The chemistry of atmosphere-forest exchange (CAFE)
967 model - PART1: Model description and characterization, Atmos Chem Phys, 11,
968 77-101, 2011.
969 Wolfe, G. M., Crounse, J. D., Parrish, J. D., St Clair, J. M., Beaver, M. R., Paulot, F.,
970 Yoon, T. P., Wennberg, P. O., and Keutsch, F. N.: Photolysis, OH reactivity and
971 ozone reactivity of a proxy for isoprene-derived hydroperoxyenals (HPALDs), Phys
972 Chem Chem Phys, 14, 7276-7286, 2012.
973 Wolfe, G. M., Cantrell, C., Kim, S., Mauldin, R., Karl, T., Harley, P., Turnipseed, A.,
974 Zheng, W., Flocke, F., Apel, E., Hornbrook, R. S., Hall, S., Ullmann, K., Henry, S.
975 B., Digangi, J., Boyle, E. S., Kaser, L., Schnitzhofer, R., Hansel, A., Graus, M.,
976 Nakashima, Y., Kajii, Y., Guenther, A., and Keutsch, F.: Missing peroxy radical
977 sources within a rural forest canopy, Atmospheric Chemistry and Physics
978 Discussion, 13, 31713-31759, 2013.
979 Wong, K. W., Tsai, C., Lefer, B., Haman, C., Grossberg, N., Brune, W. H., Ren, X.,
980 Luke, W., and Stutz, J.: Daytime HONO vertical gradients during SHARP 2009 in
981 Houston, TX, Atmos Chem Phys, 12, 635-652, Doi 10.5194/Acp-12-635-2012,
982 2012.
983 Xing, J., Wang, S. X., Jang, C., Zhu, Y., and Hao, J. M.: Nonlinear response of ozone to
984 precursor emission changes in China: a modeling study using response surface
985 methodology, Atmos Chem Phys, 11, 5027-5044, Doi 10.5194/Acp-11-5027-2011,
986 2011.
987 Yoshino, A., Nakashima, Y., Miyazaki, K., Kato, S., Suthawaree, J., Shimo, N.,
988 Matsunaga, S., Chatani, S., Apel, E., Greenberg, J., Guenther, A., Ueno, H., Sasaki,
989 H., Hoshi, J., Yokota, H., Ishii, K., and Kajii, Y.: Air quality diagnosis from
990 comprehensive observations of total OH reactivity and reactive trace species in
991 urban central Tokyo, Atmos Environ, 49, 51-59, Doi
992 10.1016/J.Atmosenv.2011.12.029, 2012.
993 Yuan, B., Warneke, C., Shao, M., and de Gouw, J. A.: Interpretation of volatile organic
994 compound measurements by proton-transfer-reaction mass spectrometry over the
995 deepwater horizon oil spill, International Journal of Mass Spectrometry, 358, 43-48,
996 Doi 10.1016/J.Ijms.2013.11.006, 2014.
997 Zhang, Y., Hu, X. M., Leung, L. R., and Gustafson, W. I.: Impacts of regional climate
998 change on biogenic emissions and air quality, J Geophys Res-Atmos, 113, Artn
999 D18310
1000 Doi 10.1029/2008jd009965, 2008a.
1001 Zhang, Y. H., Su, H., Zhong, L. J., Cheng, Y. F., Zeng, L. M., Wang, X. S., Xiang, Y. R.,
1002 Wang, J. L., Gao, D. F., Shao, M., Fan, S. J., and Liu, S. C.: Regional ozone
1003 pollution and observation-based approach for analyzing ozone-precursor
1004 relationship during the PRIDE-PRD2004 campaign, Atmos Environ, 42, 6203-
1005 6218, Doi 10.1016/J.Atmosenv.2008.05.002, 2008b.

Zhao, J., and Zhang, R. Y.: Proton transfer reaction rate constants between hydronium ion (H3O(+)) and volatile organic compounds, Atmos Environ, 38, 2177-2185, 2004.

Zhou, X. L., Zhang, N., TerAvest, M., Tang, D., Hou, J., Bertman, S., Alaghmand, M., Shepson, P. B., Carroll, M. A., Griffith, S., Dusanter, S., and Stevens, P. S.: Nitric acid photolysis on forest canopy surface as a source for tropospheric nitrous acid, Nat Geosci, 4, 440-443, 2011.

Saewung Kim 3/26/2015 4:36 PM
Deleted:

1015

1016 Table 1. Analytical characteristics of trace gas analyzers at TRF

1017

Chemical Species	Manufacturer and Model Number	Uncertainty	Lower Limit of Detection
CO	Thermo Scientific 48i TLE	10%	40 ppb
NO_X	Thermo Scientific 42i-TL with a Mo-converter	15%	50 ppt
SO_2	Thermo Scientific 43i-TLE	10%	50 ppt
ozone	Thermo Scientific 49i	5%	< 1 ppb

1018
1019

Table 2. Terpenoid speciation analysis results from GC-MS a) branch enclosure and b) ambient air samples.

a)

Terpenoids	*Composition(%)	Speciation	*Composition(%)
Isoprene	0.5		
Monoterpenes	92.9	α-pinene	36.7
		camphene	13.1
		β-pinene	12.0
		β-myrcene	27.7
		α-terpinolene	1.9
		d-limonene	8.6
Sesquiterpenes	6.6	β-caryophyllene	53.2
		α-caryophyllene	46.8

b)

Terpeniods	*Composition(%)	Speciation	*Composition(%)
Monoterpenes	98.6	α-pinene	38.8
		β-piene	36.5
		camphene	13.5
		d-limonene	11
Sesquiterpenes	1.4	longifolene	100

*Composition is calculated based on the mixing ratio scale

Table 3. A summary of critical differences in input parameters for four different model simulation scenarios presented in this study. The isoprene chemical scheme is based on Archibald et al. (2010a).

	HPALD chemistry	Observational Constraints
Scenario I	No	-All
Scenario II	#Peeters and Muller (2010)	-All
Scenario III	+Crounse et al. (2011)	-All
Scenario IV	No	-All but HONO

#k298 = ~ 0.08 for isoprene peroxy radical isomerization rate leading to produce HPALD, +k298 = 0.002 for isoprene peroxy radical isomerization rate, -All the observed diurnal variations, appeared in Figure 1 are constrained in the model along with ambient pressure and humidity.

Table 4 A summary for radical distributions from the observationally constrained box-model simulation results

	OH		HO_2		RO_2		Constraints
Local Time	8:00-12:00	13:00-16:00	8:00-12:00	13:00-16:00	8:00-12:00	13:00-16:00	
Scenario I	3.85×10^{6}	3.08×10^{6}	4.10×10^{8}	7.02×10^{8}	3.65×10^{8}	1.14×10^{9}	All
Scenario II	3.99×10^{6}	3.69×10^{6}	3.99×10^{8}	7.86×10^{8}	3.51×10^{8}	9.62×10^{8}	All
Scenario III	3.86×10^{6}	3.13×10^{6}	4.09×10^{8}	7.09×10^{8}	3.64×10^{8}	1.12×10^{9}	All
Scenario IV	1.61×10^{6}	1.61×10^{6}	1.95×10^{8}	4.82×10^{8}	1.75×10^{8}	7.25×10^{8}	All but HONO

unit: molecules cm^{-3}

Figure 1. Averaged temporal variations observed trace gases and ambient temperature at TRF (June 1st to June 6th, 2012, KST stands for Korean Standard Time GMT+9). The uncertainty for each observable is listed in the main text.

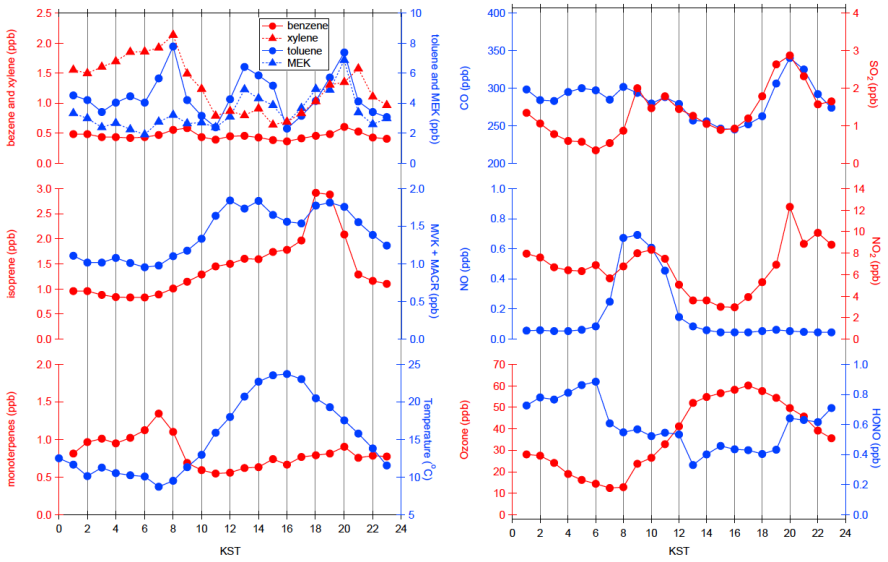

Figure 2. The temporal variations of OH reactivity calculated from the observed dataset at TRF (Figure 1).

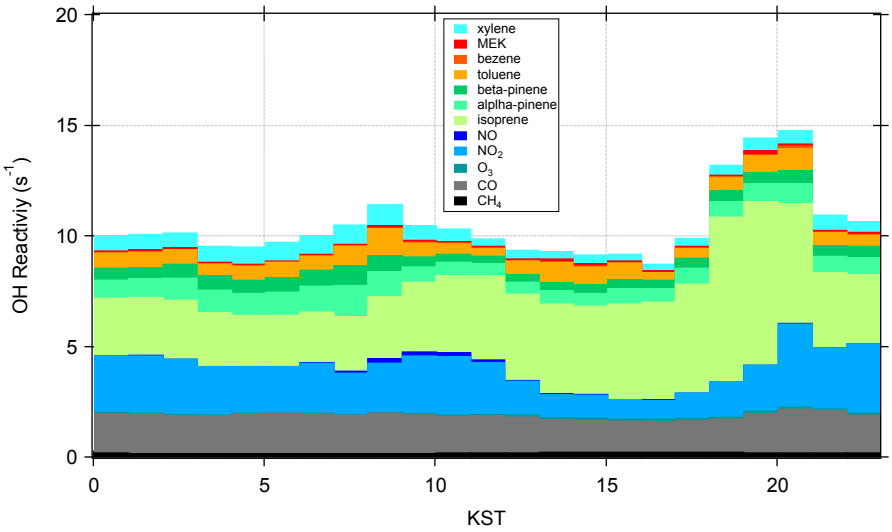

Figure 3. The temporal variations of OH (a), HO_2 (b) , and RO_2 (c) calculated by four different observationally constrained UWCM box model scenarios.

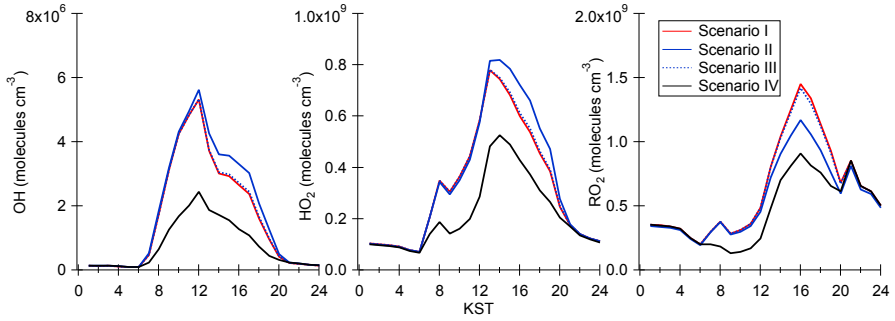

Figure 4 The temporal variations of radical recycling (red) and destruction (blue, black and green) rates calculated using the UWCM box model for different model scenarios

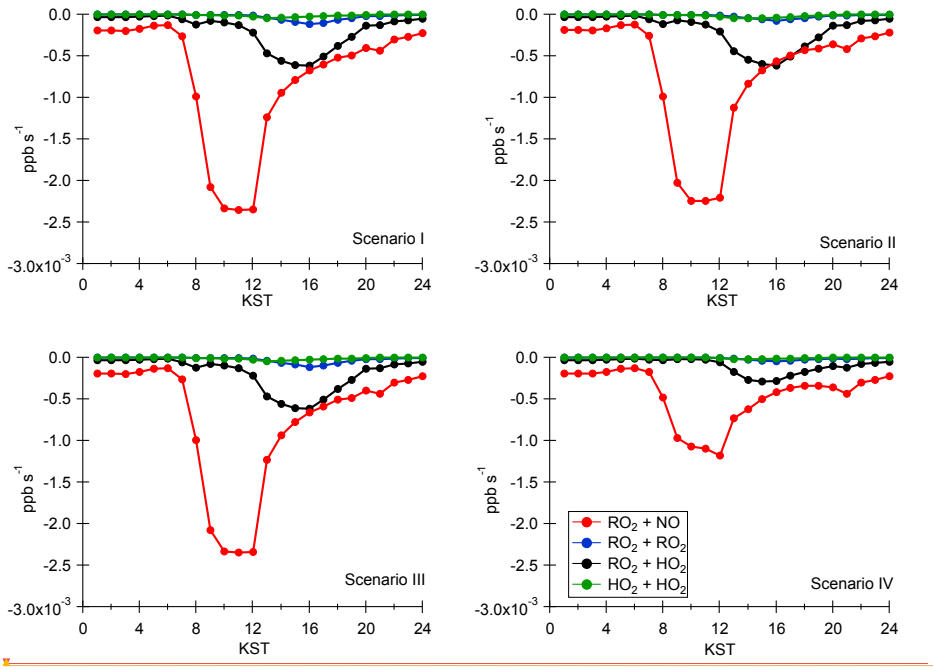

Saewung Kim 3/26/2015 9:37 AM

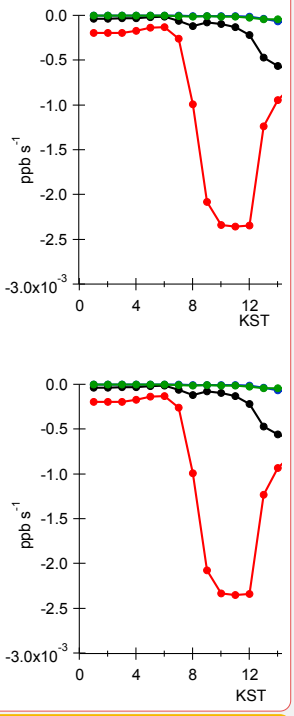

Deleted:

Unknown

Formatted: Font:(Default) Times New Roman

Figure 5. The temporal variations of P_{H2O2}/P_{HNO3} calculated from the UWCM box model from four different model scenarios

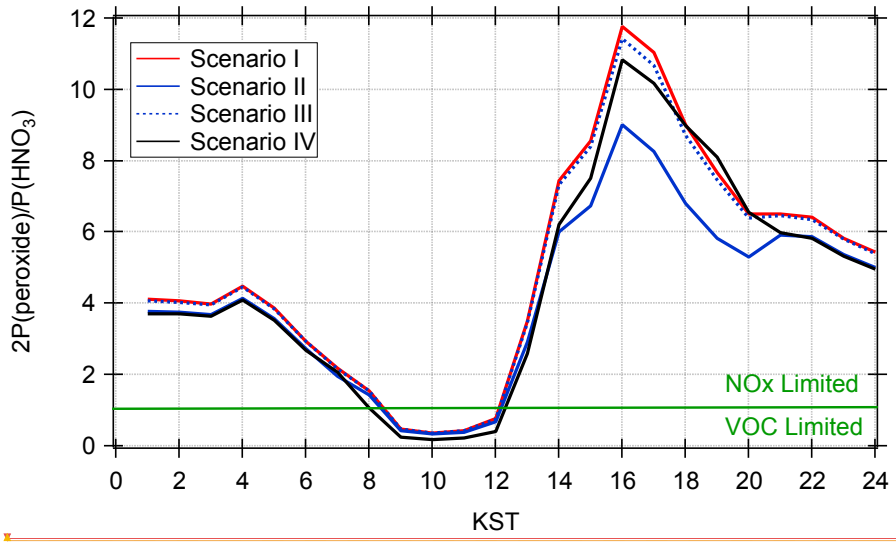

Saewung Kim 3/26/2015 9:37 AM

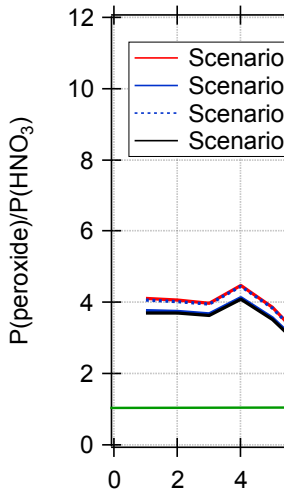

Deleted:

Unknown

Formatted: Font:(Default) Times New Roman

Figure 6. The temporal distributions of UWCM calculated OH reactivity (a) and formaldehyde (b) from different model calculation scenarios